Available online at www.sciencedirect.com
ScienceDirect
Journal of Power Sources 172 (2007) 278–286
JOURNAL OF POWER SOURCES
www.elsevier.com/locate/jpowsour

Preparation and operation of gas diffusion electrodes for high-temperature proton exchange membrane fuel cells

Chao Pan [a], Qingfeng Li [a,*], Jens Oluf Jensen [a], Ronghuan He [b], Lars N. Cleemann [a], Morten S. Nilsson [c], Niels J. Bjerrum [a], Qingxue Zeng [a]

[a] *The Materials Science Group, Department of Chemistry, Building 207, Technical University of Denmark, DK-2800 Lyngby, Denmark*
[b] *Department of Chemistry, Box 332, Northeastern University, 110004 Shenyang, China*
[c] *Danish Power Systems ApS, Raadhusvej 59, DK 2920 Charlottenlund, Denmark*

Received 9 March 2007; received in revised form 12 June 2007; accepted 8 July 2007
Available online 17 July 2007

Abstract

Gas diffusion electrodes for high-temperature PEMFC based on acid-doped polybenzimidazole membranes were prepared by a tape-casting method. The overall porosity of the electrodes was tailored in a range from 38% to 59% by introducing porogens into the supporting and/or catalyst layers. The investigated porogens include volatile ammonium oxalate, carbonate and acetate and acid-soluble zinc oxide, among which are ammonium oxalate and ZnO more effective in improving the overall electrode porosity. Effects of the electrode porosity on the fuel cell performance were investigated in terms of the cathodic limiting current density and minimum air stoichiometry, anodic limiting current and hydrogen utilization, as well as operations under different pressures and temperatures.

Keywords: Gas diffusion electrode; Polybenzimidazole; Phosphoric acid; Proton exchange membrane fuel cell; Electrode porosity

1. Introduction

As the most important part of proton exchange membrane fuel cells (PEMFCs), the membrane–electrode-assembly (MEA) is consisting of a proton exchange membrane as electrolyte and two gas diffusion electrodes attached on each side of the membrane. In order to improve the MEA or PEMFC performance, great efforts have been made to develop both materials and technologies for the membrane and electrodes.

The currently well-developed PEMFC technology is based on perfluorosulfonic acid (PFSA) polymer membranes (e.g., Nafion) as electrolyte [1]. The perfluorinated backbone gives these materials excellent long-term stability in both oxidative and reductive environments, while the sulfonic acid terminal groups provide the materials high proton conductivity. The conductivity, however, is dependent on the presence of water to solvate the protons from the sulfonic acid groups. As a consequence the operational temperature is limited to be below 100 °C, typically 80 °C, under atmospheric pressure. The new development of this field is temperature-resistant membranes for operation above 100 °C [2]. With acid-doped polybenzimidazole (PBI) membranes [3], high-temperature PEMFC has been demonstrated with operating features such as little or no humidification, high CO tolerance, better heat utilization and possible integration with fuel processing units [4–6].

The state-of-the-art of electrocatalysts for PEMFC, on the other hand, has been based on noble metals supported on carbon blacks (Pt/C), in order to achieve a high degree of metal dispersion and reduction in noble metal loading and cost. The carbon blacks with high surface area in a range of $(4–6) \times 10^8\ m^2$ per cubic meter bulk volume, corresponding to a specific surface area of 200–250 $m^2\ g^{-1}$ seem the best candidates, with Vulcan XC-72 as a typical example.

For preparing MEAs, the catalysts are typically applied on the membrane in two ways: application of the catalyst onto a gas diffusion layer (GDL) followed by membrane addition, or application of the catalyst to the membrane followed by GDL attachment. In both cases, an assembly of membrane, catalyst and GDL is finally made by hot-pressing.

* Corresponding author. Tel.: +45 45 25 23 18; fax: +45 45 88 31 36.
E-mail address: lqf@kemi.dtu.dk (Q. Li).

0378-7753/$ – see front matter © 2007 Elsevier B.V. All rights reserved.
doi:10.1016/j.jpowsour.2007.07.019

Application of catalysts onto GDL is a method similar to the technology for preparing phosphoric acid fuel cell electrodes, where polytetrafluoroethylene (PTFE) is used as the catalyst binder, to make the catalyst layer hydrophobic and therefore allow both liquid acid and reactant gases to access the active sites of the catalyst. In this way a network structure of a three-phase zone is established, consisting of a proton-conducting electrolyte, electron-conducting catalysts, and reactant gases. As a comparison, for PEMFC electrodes, a key issue is to improve the protonic access to the majority of catalyst sites not in intimate contact with the membrane [7]. A historical invention [8] was to impregnate the active layer of the porous gas diffusion electrode with the proton-conducting polymer in order to extend the three-phase zone.

Different techniques of gas diffusion electrode fabrication have been developed, for example, by dry rolling of a mixture of Pt/C and PTFE [9], spraying of a mixture of water, alcohol, and colloidal PTFE and Pt/C [9], depositing [10] or casting of a slurry [4]. Another way is to impregnate the GDL first with an ionomer. Taylor et al. [11] impregnated the porous carbon structure with a solubilized PFSA in a mixture of lower aliphatic alcohols and water and then deposited platinum onto the carbon support electrochemically. All these developments are based on PFSA membranes.

For PBI-based membranes, little effort has been made to fabricate gas diffusion electrodes, compared with other types of fuel cells such as phosphoric acid fuel cells or Nafion-based polymer membrane electrolyte fuel cells. In the earlier works to develop PBI cells, Wang et al. [12] used phosphoric acid fuel cell electrodes treated by impregnation with the PBI polymer. The group has also tried to use platinum black and platinum–ruthenium alloy for manufacturing cathode and anode by a filtering-pressing method, at a rather high loading of noble metal catalysts (4 mg cm^{-2}) [13]. A spraying method was developed with the ink of catalyst particles dispersed in PBI solution in DMAc by Tunold's group [14]. A mixture of Pt/C and PBI solution in *N*-methylpyrrolidone (NMP) has also been used for spraying [15].

In our group, the gas diffusion electrodes have been prepared by a tape-casting method with PBI as the catalyst binder [16]. For the purpose of tape-casting, a stiff GDL material was used. To smooth the surface of the wet-proofed carbon paper, a supporting layer of PTFE-bonded carbon black is first cast. Finally a slurry of Pt/C catalysts in a PBI solution was applied on the top of the supporting layer. Here the PBI polymer is used both as the binder for the catalysts and as the proton conductor after the acid impregnation.

When PBI is used as binder, the catalyst layer appears dense compared with those that are bonded with either Nafion or PTFE as binder. The PBI electrodes perform well with oxygen as the oxidant. When it is switched from oxygen to air, however, a larger performance loss occurs. In the present work, efforts are made to improve the tape-cast PBI electrodes with tailored porosities by introducing porogens in both the gas diffusion layer and the catalyst layer. The performance of electrodes with varied porosities was investigated at temperatures up to 200 °C and pressures of up to 4 bar with different compositions of fuel and oxidant gases.

2. Experimental

2.1. Gas diffusion layer

The carbon fiber paper, Toray TGP-H-120 (Toray Co.), was employed as the GDL. For wet-proofing, the carbon paper was immersed in a PTFE dispersion (Du Pont) of different concentrations for about 10 min. After drying in air at room temperature overnight, the carbon paper was sintered in air at 360 °C for 15 min.

2.2. Supporting layer

In order to smooth the GDL surface and therefore avoid cracking of the catalyst layer, a supporting layer of PTFE-bonded carbon blacks was applied to the wet-proofed GDL. For doing so, a solution of 18% poly(vinyl butyral) (PVB, Aldrich) in xylene (Aldrich) was prepared as solvent. The PTFE dispersion was first mixed with a plasticizer (Santicizer® 160, Monsanto Europe S. A.), and then added to the PVB–xylene solvent under stirring. Carbon black (VXC 72R, Cabot) in a weight ratio of 6:4 to the PTFE content was finally added and mixed thoroughly. In case a porogen is used, it was always added as the last to the slurry. The slurry was applied onto the wet-proofed carbon paper by tape-casting, dried at room temperature overnight, followed by sintering at 360 °C for 20 min.

2.3. Catalyst layer

Twenty weight percent of Pt/C powders were mixed with a 7 wt% PBI solution in DMAc (*N*,*N*-dimethylacetamide, Sigma–Aldrich). The loading of Pt and PBI was about 0.5 and 0.7 mg cm^{-2}, respectively. The mixture was applied on the top of supporting paper by tape-casting, dried first at room temperature overnight and finally at 200 °C for 3 h. In case the ammonium oxalate was used as an additive, the catalyst layer was finally heated at 265 °C for 2 h. Thus prepared gas diffusion electrodes consist of a wet-proofed carbon paper as GDL, a carbon supporting layer and a catalyst layer.

2.4. Acid impregnation

A 10 wt% phosphoric acid was sprayed on the catalyst layer surface of the electrodes, in order to protonate the PBI binder. The molar ratio of the acid and the PBI content in the catalyst layer was about 12–15:1. After drying at about 120 °C for an hour, the gas diffusion electrode was ready for preparing MEAs.

2.5. Porogens

In order to tailor the porosity of the gas diffusion electrodes, i.e. the carbon supporting layer and the catalyst layer, a few porogens were selected as additives to the supporting layer and/or the catalyst layer slurries. The porogens should be either volatile

or soluble so that they could afterwards be removed by heating or washing/leaching. The selected porogens in this study included ammonium oxalate, ammonium carbonate, ammonium acetate and zinc oxide. The thermal stability of these ammonium salts was first examined by thermogravimetric analysis (TGA, NETZSCH, STA 409 PC) in a temperature range from room temperature to 300 °C at a heating rate of 3 °C min^{-1} in air.

2.6. Porosity measurements

The wet-proofed GDL, GDL with the supporting carbon layer, and the overall electrode (GDL plus supporting layer and catalyst layer) are, to some extent, hydrophobic due to the presence of PTFE. Organic liquid, for example, toluene, can however wet and fill the micropores of thee materials. A method to determine the porosity by using an organic liquid suggested by Wendt and co-workers [17] was modified as follows. A sample of electrode, with pre-measured weight, size and thickness (the thickness is given as an average of at least 20 measurements at different places), was contained in a necked flask. After applying vacuum for 30 min, liquid toluene was injected into the flask using a syringe. After 10 min of saturation the electrode sample was quickly taken out of the liquid toluene, transferred into a pre-weighed bottle and covered with a cap, and weighed. The quantity of toluene in the pores of the sample was obtained from the weight change of the sample after and before the toluene sucking. The pore volume in the sample and therefore the electrode porosity were then calculated from the weight and density of toluene.

2.7. PBI membranes and MEA

PBI membranes were prepared from 5 wt% of PBI solution in *N*,*N*-dimethylacetamide (DMAc). After drying at temperatures of up to 120 °C, the obtained membranes were further pre-treated by first washing with hot water, followed by heating at 190 °C for 2 h. For doping with phosphoric acid, the membranes were immersed in 75% acid solution for at least 7 days at room temperature. This gives the membrane an acid doping level of about 6.0 mol H_3PO_4 per repeat unit of the polymer. The acid-doped membrane was then sandwiched between two gas diffusion electrodes on each side and hot-pressed under a pressure of about 10 MPa at 150 °C for 10 min.

2.8. Fuel cell test

A single test cell with an active electrode area of 5 cm × 5 cm was constructed with two graphite plates. The gas channels on the graphite plates were made in simple parallel grooves of 2 mm width and 1 mm depth with ribs that were 1 mm wide. Two stainless steel end plates with attached heaters were employed to clamp the graphite plates and collect the current. The flow rates and pressures of the reactant gases, oxygen, air, hydrogen, and pre-mixed 75% H_2–25% CO_2, were controlled with electronic mass flow controllers (Brooks Instrument-0154) and backpressure regulators (Pressure Controller, Brooks Instrument-5866). Both hydrogen and air were used as dry gases, directly from the compressed bottles without pre-humidification. Polarization curves were obtained by a current step potentiometry with the steady state potential recorded 2 min after each current was set. All polarization curve was measured beginning with the highest currents.

3. Results and discussion

3.1. TGA of porogens

The TGA curves of three studied ammonium salts are shown in Fig. 1. The decomposition of ammonium carbonate starts at temperatures of about 60 °C and completes at above 130 °C. The decomposition of ammonium acetate is observed in a temperature range from 80 °C to 160 °C. For ammonium oxalate, after predrying at 120 °C for 2 h, the decomposition occurs at temperatures above 180 °C and is complete above 260 °C.

For preparing carbon supporting layers, the sintering temperature should be higher than the melting point of PTFE, i.e. above 330 °C. At that temperature, all these ammonium salts will be decomposed. For preparing the catalyst layer with the ammonium acetate and carbonate as porogens, the drying temperature was around 200 °C, however, when the ammonium oxalate was used as the porogen, a drying temperature of 265 °C was used.

In addition, ZnO was only tested as additive to the supporting layer. After sintering of the supporting layer, ZnO was removed by immersing the sample in 2 M H_2SO_4 at 70 °C for 30 min, followed by thoroughly washing with deionized water.

3.2. Porosity of wet-proofed GDL

Wet-proofing of the carbon fiber paper is performed in order to provide hydrophobicity, however, this is obtained at the expense of decreased porosity, and electronic conductivity as well. By saturating the carbon fiber paper in the PTFE dispersion of different concentrations, the porosity and the PTFE loading of the carbon paper changed accordingly. Fig. 2 shows the correlation of the porosity and the PTFE loading as a result of the concentration of PTFE dispersions. The measured porosity of pristine samples was 77.3%, in good agreement with the reported porosity of 78% by the supplier.

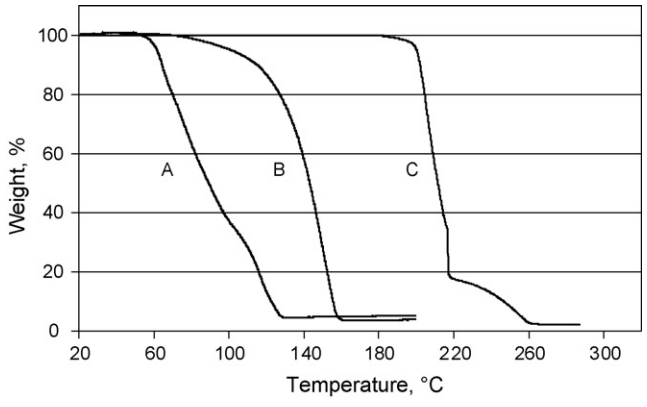

Fig. 1. Thermogravimetric analysis (TGA) of additives to gas diffusion electrodes. (A) $(NH_4)_2CO_3$; (B) CH_3COONH_4; (C) $(COONH_4)_2$.

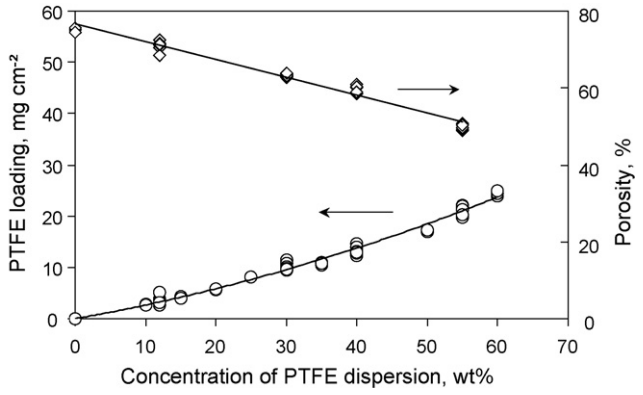

Fig. 2. The porosity and the PTFE loading of the gas diffusion layer materials treated in the PTFE suspension of different concentrations.

The surface morphologies of the carbon paper before and after wet-proofing with PTFE are examined by scanning electron microscopy (SEM), as shown in Fig. 3. The surface profile of initial carbon fibers and irregular pores are seen in Fig. 3A. By increasing the concentration of the dispersion, the PTFE loading on the treated carbon fiber paper increases and the porosity decreases. As seen from Fig. 3, the PTFE, after sintering, is covering the carbon fiber surface. At higher loadings, it also fills up the corners, i.e. the small pores, created by the crossing of carbon fibers. This will improve the mechanical strength of the carbon paper.

The PTFE loading in the GDL is a compromise of increased hydrophobicity and strength on one side and decreased porosity and conductivity on the other. For phosphoric acid fuel cells (PAFC) where an essentially liquid electrolyte is present in a PTFE-bonded matrix, typically made of SiC, the hydrophobicity of the gas diffusion electrodes is of special importance for establishing the three-phase zone. As a consequence, high PTFE loadings (of a PTFE-to-Pt/C ratio around 4/6) are generally used.

Considering that the involved water is in vapor form at the operational temperatures of the PBI cell in this work, the problems associated with the presence of liquid water are negligible. A high porosity of the gas diffusion layer for gas transfer is preferred. Therefore a PTFE dispersion of 12 wt% was used to pre-treat the carbon paper giving a corresponding porosity of the gas diffusion layer of about 70%.

3.3. The influence of porogens on the porosity of gas diffusion electrodes

By introducing porogens in the supporting layer and the catalyst layer, the porosity of the gas diffusion layer plus supporting layer and the overall porosity of the gas diffusion electrodes (gas diffusion layer plus supporting and catalysts layers) were measured. For these studies, all the gas diffusion layers were wet-proofed with 12% PTFE dispersion.

The porosity variation of GDL with supporting layers prepared from a slurry with and without porogens is shown in Fig. 4. Without any porogens in the supporting layer slurry, the porosity of the gas diffusion layer was found to be in a range of 42–44%. With the help of porogens, the porosity of the gas diffusion layers was found to increase. With about 4 wt% of ammonia oxalate in the casting slurry, up to 62% of porosity was achieved. With ZnO, the porosity of over 60% was obtained. By introducing ammonium carbonate and acetate, improvements in the porosity, being over 50%, were also observed.

In the following studies, the GDL with supporting layer having an overall porosity of 62%, prepared by using ammonium oxalate as porogen, was used for fabrication of the gas diffusion electrodes. On top of the supporting layer a catalyst layer was cast from catalyst slurries containing various amounts of ammonium oxalate as porogen and the overall porosity of the gas diffusion electrodes was measured. This overall porosity of the gas diffusion electrodes was an average porosity of the GDL, supporting layer and catalyst layer, as shown in Fig. 5. Without using porogen in the catalyst layer, the overall porosity of the gas diffusion electrode was about 50%. By using ammonium oxalate at a content of up to 30 wt% in the catalyst slurry, the overall porosity was increased by more than 8%. As the ammonium salt is removed as gases at elevated temperatures, some cracks or larger pores were formed in the electrode structure, as seen from the SEM images in Fig. 5, allowing gas to pass through. Those parts without cracks appear similar to the electrodes without addition of porogens.

3.4. Electrode porosity and fuel cell performance

Gas diffusion electrodes were prepared with the overall porosity varying from 38% to 59%, based on which PBI cells were constructed and tested under atmospheric pressure. The used PBI membranes were doped with 6.0 mol phosphoric acid and the catalyst loading was 0.5 mg Pt cm^{-2} for both electrodes. The used fuels were pure hydrogen and hydrogen containing 25% CO_2 and the oxidant was pure oxygen or air. A set of polarization curves obtained at 200 °C are shown in Fig. 6, where the oxygen and air flow rates were 400 ml min^{-1} and 800 ml min^{-1}, respectively, not, however, in the same oxygen stoichiometry.

It is seen that the cell performance with electrodes of different porosities is different, especially when the cell is operated at high current densities. It is obvious that under these conditions the electrode processes are limited predominantly by the gaseous mass transportation. It is interesting to notice that the electrode structures with a high porosity do not seem to sacrifice the catalytic activities. Similar results have been reported [18–20]. Yan et al. [18] reported that a gas diffusion layer of higher porosity has an ability of better mass transportation, which is beneficial in that it supplements the reactant gas to the catalyst layer and thus shifts the occurrence of the performance drop to a higher value of the current density. Chu et al. [19] studied the influence of the porosity of the gas diffusion layer on the performance of a Nafion-based PEM fuel cell. Their results also showed that a fuel cell generally exhibits better performance when a gas diffusion layer of higher porosities is used. As seen from their results, a change in the porosity of the gas diffusion layer has virtually no influence on the polarization when the current density is in a low or medium range, though a better performance is achieved when the current density is close to the limiting value.

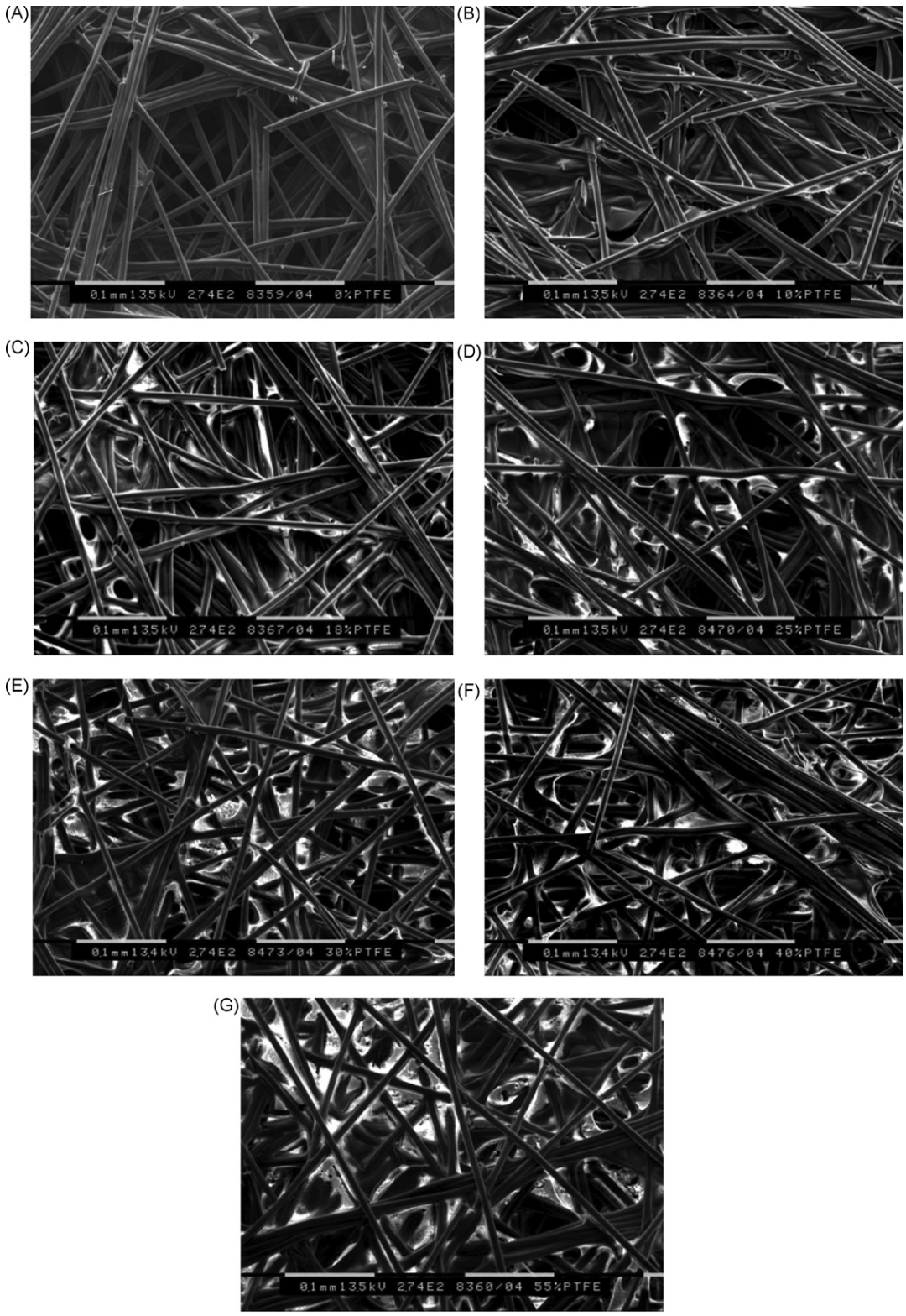

Fig. 3. SEM pictures of carbon papers treated by PTFE solutions with a weight concentration of (A) 0% PTFE, (B) 10% PTFE, (C) 18% PTFE, (D) 25% PTFE, (E) 30% PTFE, (F) 40% PTFE and (G) 55% PTFE.

The fuel cell polarization at low and medium current densities was dominated by activation losses and ohmic losses. The activation losses were decided by the cell temperature, catalyst activity, reactant concentration and the pressure. The ohmic losses were decided by the electrical resistance of the electrodes and the resistance to the flow of ions in the electrolyte. The effect of improved porosity is therefore significant only at high current densities where the mass transportation is limiting the process.

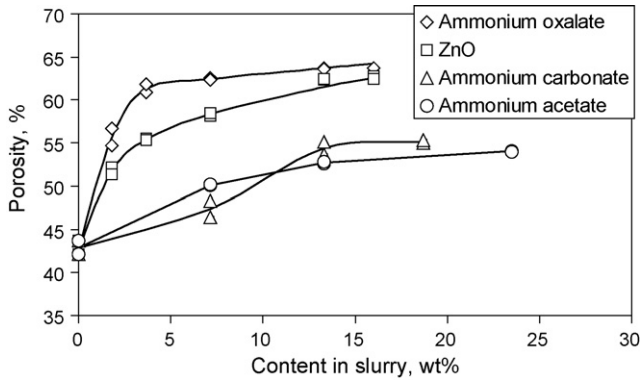

Fig. 4. Porosity of the gas diffusion layer plus a carbon supporting layer as a function of the porogen content in the supporting layer slurry.

3.5. Cathode limiting current and air stoichiometry

Fig. 7 shows a set of polarization curves of a PBI cell with electrodes of 59% overall porosity operating with hydrogen and air at 200 °C. At the anode side the hydrogen flow was set at 400 ml min^{-1}, whereas the air flow at the cathodic side varied from 100 ml min^{-1} to 1000 ml min^{-1} (the active area of the electrode was 25 cm^2). In the low current density range, no significant changes in the polarization curves occurred, as expected. For the measurements with low flow rates of air, limiting currents due to the mass transportation limitation were clearly observed.

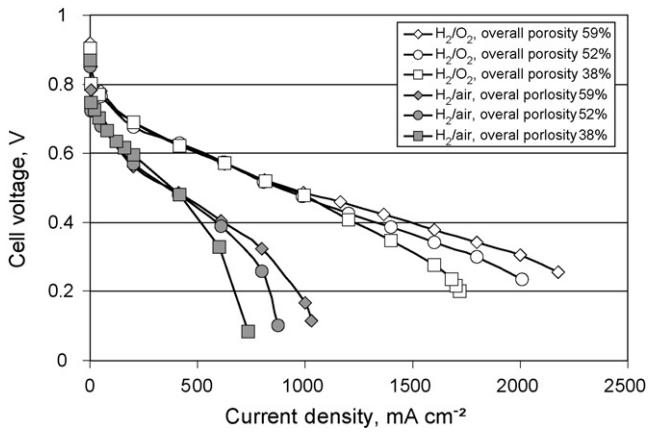

Fig. 6. Polarization curves of a PBI fuel cell with electrodes of different porosities operating with dry gases at atmospheric pressure. Platinum loading of the electrode was 0.5 mg Pt cm^{-2} and the active area of the electrode was 25 cm^2. Hydrogen and oxygen flow rates were 400 ml min^{-1} and the air flow rate was 800 ml min^{-1}.

Similar results were obtained for electrodes of lower overall porosity (38%), where the limiting currents occurred at a much lower value than that for electrodes of higher porosity.

A critical current density is defined as the value at which a significant deviation of the polarization curves from the nearly linear voltage–current density relationship started. For each air flow rate, a theoretical maximum current density can be calcu-

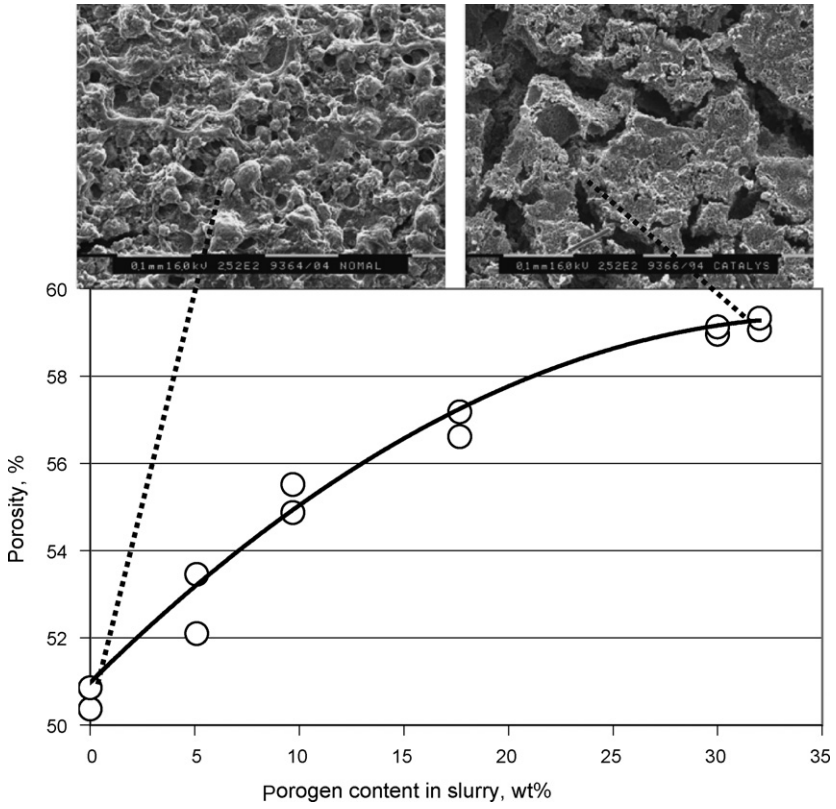

Fig. 5. The overall porosity of the gas diffusion electrodes as a function of the porogen content in the catalyst slurry. The initial porosity of the gas diffusion layer was 62%. The catalyst layer contained 0.5 mg Pt cm^{-2} and 0.7 mg PBI cm^{-2}. The SEM images are for the catalyst layer without using porogen (overall porosity of 38%, to left) and for the catalyst layer with porogen (overall porosity of 59%, right).

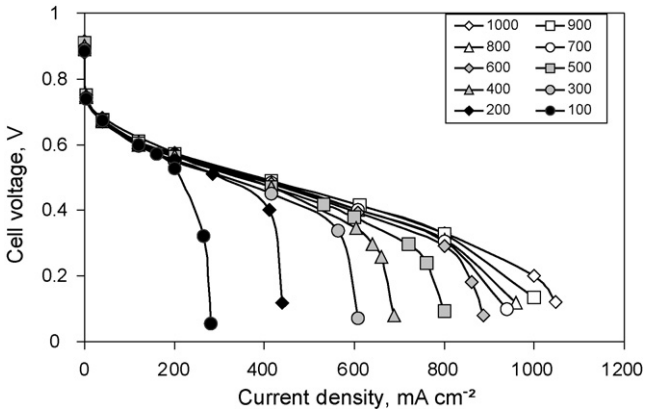

Fig. 7. Polarization curves of a PBI cell with electrodes of 59% overall porosity operating with dry hydrogen and air at 200 °C. The hydrogen flow was 400 ml min^{-1} whereas the air flow was varied, as indicated in the figure (in ml min^{-1}). The active area of electrodes was 25 cm^2.

lated using Faraday's law. The ratio of the theoretical maximum current density to the measured critical current density is in fact the minimum air stoichiometry (lamda), where a mass transportation of gaseous oxygen molecules through the gas diffusion electrode starts to dominate the electrode process. The minimum air stoichiometry (lamda) is apparently a function of the electrode structure and the operating current density. Fig. 8 shows the correlation of the minimum lamda with the critical current density for two types of electrodes with overall porosity being 38% and 59%, respectively. At a lamda of 2, the electrodes with 59% overall porosity can reach a critical current density as high as 800 mA cm^{-2} whereas for the electrode with 38% overall porosity it is only about 200 mA cm^{-2}. It is also seen that with electrodes of high porosity, the fuel cell can operate at the air stoichiometry close to 1 without significant loss of performance, whereas with electrodes of low porosity, a lamda of above 2 seems necessary. In the latter case, at very low current densities, the total gas flow is very small, giving poor purging effect. As a result, the minimum lamda seems slightly higher at very low operating current densities.

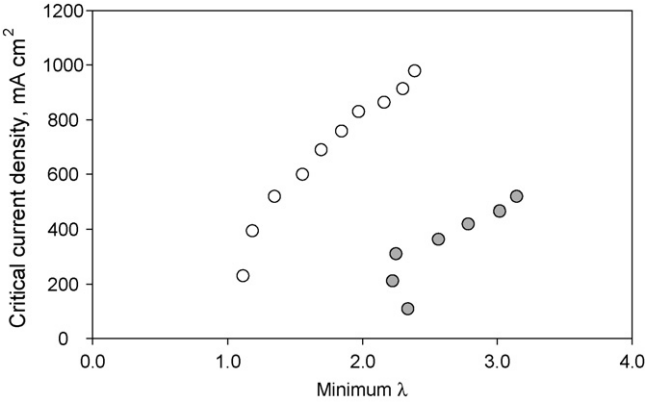

Fig. 8. The cathodic critical current density as a function of the minimum stoichiometry (lamda) of air for two types of gas diffusion electrodes with overall porosity being 38 (filled cycles) and 59% (open cycles), respectively.

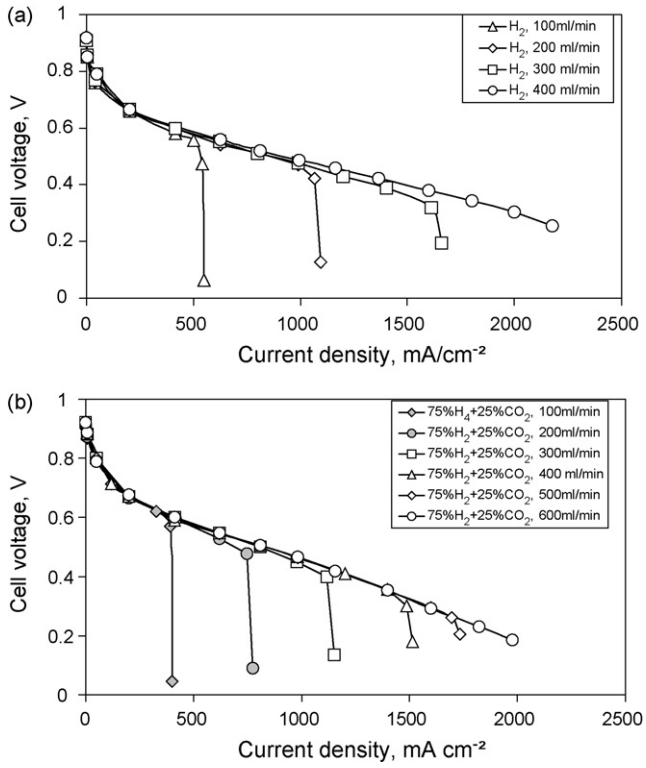

Fig. 9. Polarization curves of a PBI cell with electrodes of 59% overall porosity operating with dry oxygen at 200 °C. The oxygen flow was 400 ml min^{-1} whereas the fuel feed was either pure hydrogen (a) and hydrogen containing 25% CO_2 (b). The fuel flow rates are indicated in the figure (in ml min^{-1}). The active area of electrodes was 25 cm^2.

3.6. Anodic limiting current and hydrogen utilization

Fig. 9 shows polarization curves of a PBI cell with electrodes of 59% overall porosity operating at 200 °C. The oxidant was pure oxygen at a flow rate of 400 ml min^{-1}. The fuel was either pure hydrogen or hydrogen containing 25% CO_2. In the low current density range, the fuel cell performance is very much similar for hydrogen and hydrogen containing carbon dioxide. At higher current densities, the polarization curves have the same behaviour. Taking into account of the low hydrogen content in the hydrogen and carbon dioxide mixtures, the limiting current densities at the same overall gas flow rate give nearly the same fuel utilization.

From the obtained limiting currents at each flow rate, the utilization of hydrogen is calculated for both pure hydrogen and hydrogen containing carbon dioxide as fuel, as shown in Fig. 10. Higher utilization of hydrogen is achieved for pure hydrogen than for hydrogen–CO_2 mixtures. By increasing the overall porosity of electrodes, the fuel utilization at the limiting current density also improves. At a fuel gas flow rate of 300 ml min^{-1}, the hydrogen utilization was about 94%, 97% and 99% for electrodes of overall porosity of 38%, 52% and 59%. When hydrogen containing 25% CO_2 was used as fuel, the hydrogen utilization was about 86%, 87% and 89%, respectively. At higher gas flow rates, the difference becomes obviously larger. At low gas flow rates (below 200 ml min^{-1}), nearly 100% utilization of hydrogen can be achieved with pure hydrogen,

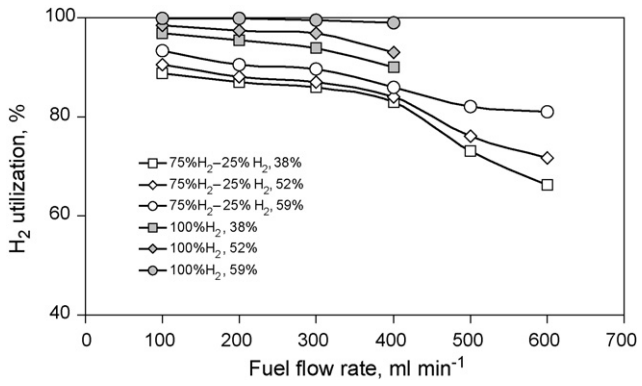

Fig. 10. Hydrogen utilization at limiting current density as a function of the fuel flow rate. Both pure hydrogen and hydrogen containing 25% CO_2 were used as dry gases. The overall porosity of the studied electrodes were 38%, 52% and 59%, respectively, as indicated in the figure. The active area of electrodes was 25 cm^2.

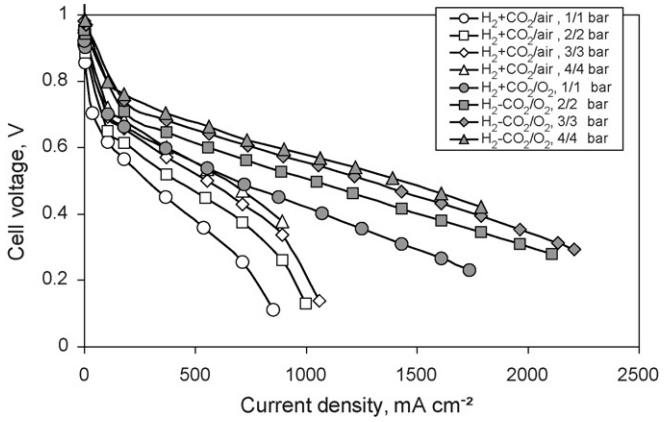

Fig. 11. Polarization curves of a PBI cell operating at 200 °C and different pressures. The electrodes had an overall porosity of 59%. The O_2 and H_2–CO_2 flow rates were 400 ml min^{-1}, and the air flow rate was 800 ml min^{-1}. The active area of electrodes was 25 cm^2.

while it is only above 90% for hydrogen containing 25% CO_2. It should be remarked that these results were achieved using graphite bipolar plates with simple parallel gas channels.

3.7. Pressure and temperature effects

Increase in the inlet concentration or partial pressure of reactants at an electrode would enhance the cell performance due to decreased concentration polarization and Nernst losses. A systematic study of the PBI cell performance under various pressures was made and summarized in Table 1, where the cell performance is expressed in term of the current density at a cell voltage of 0.5 V. With both the hydrogen and H_2–CO_2 mixture as fuel, oxygen and air as the oxidant, significant improvements in the cell performance are observed for gas diffusion electrodes of 59% overall porosity compared to electrodes of 38% overall porosity.

Table 1
Summary of the fuel cell tests at different pressures

Fuel/oxidant	Pressure (bar)	Current density (mA cm^{-2}) at cell voltage of 0.5 V	
		Electrode porosity: 38%	Electrode porosity: 59%
H_2/O_2	1/1	750	950
	1/2	950	1050
	1/3	1100	–
	2/2	1250	1368
H_2/air	1/1	250	370
	1/2	350	490
	1/3	480	–
	2/2	480	500
	3/3	620	–
$75H_2$–$25CO_2/O_2$	1/1	700	850
	1/2	–	1120
	1/3	–	1200
	2/2	1030	1350
	3/3	1280	–
	4/4	1450	–
$75H_2$–$25CO_2$/air	1/1	280	490
	1/2	480	520
	1/3	500	–
	2/2	420	650
	3/3	550	–
	4/4	650	

Fig. 11 shows a set of polarization curves obtained at different pressures for H_2–CO_2 fuel and O_2 or air at 200 °C. The overall porosity of electrodes was 59%. Significant improvement in the cell performance is observed in the pressure range from 1 bar to 4 bar.

4. Conclusions

Gas diffusion electrodes for PBI-based PEMFCs were prepared by a tape-casting method. The porosity of electrodes was tailored by introducing porogens such as ammonium oxalate, carbonate and acetate or acid-soluble oxide, e.g. ZnO into the supporting layer and/or catalyst layers. Ammonium oxalate and ZnO seem effective in improving the overall electrode porosity. An increase in the overall electrode porosity from 38% to 59% was achieved without sacrificing the catalytic activity of the electrodes. By performing fuel cell tests, significant effects of the electrode porosity were observed on the cathodic limiting current density and air stoichiometry, anodic limiting current and hydrogen utilization, as well as the pressure and temperature impacts.

Acknowledgements

This work has received financial support from the European Commission under the 6th Framework Programme (SES6-CT-2004-502782) and the Danish PSO-F&U Programme (project number 5728).

References

[1] P. Costamagna, S. Srinivasan, J. Power Sources 102 (2001), 242 and 253.
[2] Q. Li, R. He, J.O. Jensen, J. Bjerrum, Chem. Mater. 15 (2003) 4896.

[3] J.S. Wainright, J.-T. Wang, D. Weng, R.F. Savinell, M. Litt, J. Electrochem. Soc. 142 (1995) L121.
[4] Q. Li, H.A. Hjuler, N.J. Bjerrum, J. Appl. Electrochem. 31 (2001) 773.
[5] Q. Li, R. He, J.O. Jensen, N.J. Bjerrum, Fuel Cells Fundam. Syst. 4 (2004) 147.
[6] C. Pan, R. He, Q. Li, J.O. Jensen, N.J. Bjerrum, H.A. Hjulmand, A.B. Jensen, J. Power Sources 145 (2005) 392.
[7] E. Ticianelli, C. Derouin, S. Srinivasan, A. Redondo, J. Electochem. Soc. 135 (1988) 2209.
[8] I.D. Raistrick, US Patent 4,876,115 (1989).
[9] S. Srinivasan, A. Ferreira, R. Mosdale, S. Mukerjee, J. Kim, S. Hirano, S. Lee, S. Buchi, A. Appleby, Proceedings of the Fuel Cells—Program and Abstracts on the PEMFC for Space and Electric Vehicle Application, 1994, p. 424.
[10] D. Bevers, N. Wagner, Bradke, Int. J. Hydrogen Energy 23 (1998) 57.
[11] E. Taylor, E. Anderson, N. Vilambi, J. Electrochem. Soc. 139 (1992) L45.
[12] J.-T. Wang, R.F. Savinell, J. Wainright, M. Litt, H. Yu, Electrochim. Acta 41 (1996) 193.
[13] J.-T. Wang, J.S. Wairight, R.F. Savinell, M. Litt, J. Appl. Electrochem. 26 (1996) 751.
[14] F. Seland, T. Berning, B. Børresen, R. Tunold, J. Power Sources 160 (2006) 27.
[15] J. Hu, H. Zhang, Y. Zhai, G. Liu, B. Yi, Int. J. Hydrogen Energy 31 (2006) 1855.
[16] Q. Li, R. He, J.-A. Gao, J.O. Jensen, N.J. Bjerrum, J. Electrochem. Soc. 150 (2003) A1599.
[17] A. Fischer, J. Jindra, H. Wendt, J. Appl. Electrochem. 28 (1998) 277.
[18] W.M. Yan, C.Y. Soong, F. Chen, H.S. Chu, J. Power Sources 125 (2004) 27.
[19] H.-S. Chu, C. Yeh, F. Chen, J. Power Sources 103 (2003) 1.
[20] V. Gurau, F. Barbir, H. Liu, J. Electrochem. Soc. 147 (2000) 2468.